An ABCA1-independent pathway for recycling a poorly lipidated 8.1 nm apolipoprotein E particle from glia

Jianjia Fan,* Sophie Stukas,* Charmaine Wong,* Jennifer Chan,* Sharon May,* Nicole DeValle,[†] Veronica Hirsch-Reinshagen,* Anna Wilkinson,* Michael N. Oda,[†] and Cheryl L. Wellington[1],*

Department of Pathology and Laboratory Medicine,* University of British Columbia, Vancouver, British Columbia, Canada; and Children's Hospital of Oakland Research Institute,[†] Oakland, CA

Abstract Lipid transport in the brain is coordinated by glial-derived lipoproteins that contain apolipoprotein E (apoE) as their primary protein. Here we show that apoE is secreted from wild-type (WT) primary murine mixed glia as nascent lipoprotein subspecies ranging from 7.5 to 17 nm in diameter. Negative-staining electron microscopy (EM) revealed rouleaux, suggesting a discoidal structure. Potassium bromide (KBr) density gradient ultracentrifugation showed that all subspecies, except an 8.1 nm particle, were lipidated. Glia lacking the cholesterol transporter ABCA1 secreted only 8.1 nm particles, which were poorly lipidated and nondiscoidal but could accept lipids to form the full repertoire of WT apoE particles. Receptor-associated-protein (RAP)-mediated inhibition of apoE receptor function blocked appearance of the 8.1 nm species, suggesting that this particle may arise through apoE recycling. Selective deletion of the LDL receptor (LDLR) reduced the level of 8.1 nm particle production by approximately 90%, suggesting that apoE is preferentially recycled through the LDLR. Finally, apoA-I stimulated secretion of 8.1 nm particles in a dose-dependent manner. These results suggest that nascent glial apoE lipoproteins are secreted through multiple pathways and that a greater understanding of these mechanisms may be relevant to several neurological disorders.—Fan, J., S. Stukas, C. Wong, J. Chan, S. May, N. DeValle, V. Hirsch-Reinshagen, A. Wilkinson, M. N. Oda, and C. L. Wellington. **An ABCA1-independent pathway for recycling a poorly lipidated 8.1 nm apolipoprotein E particle from glia.** *J. Lipid Res.* 2011. **52:** 1605–1616.

Supplementary key words   apoE • lipoprotein • recycling

High density lipoprotein (HDL) mediates reverse cholesterol transport (RCT), which is the process by which excess cholesterol is collected from peripheral tissues and delivered to the liver for biliary excretion or to steroidogenic organs for steroid hormone biosynthesis (1). The rate-limiting step in HDL biogenesis is catalyzed by the cholesterol transporter ABCA1, which effluxes cholesterol and phospholipids from the plasma membrane to apolipoprotein acceptors (2–4). In plasma, the primary apolipoprotein acceptor for ABCA1 is apolipoprotein A-I (apoA-I), whereas in the central nervous system (CNS) it is apoE (5, 6). Deficiency of ABCA1 causes Tangier disease (TD), which is characterized by a nearly total loss of plasma HDL and increased catabolism of poorly lipidated apoA-I in the kidney (7). TD subjects also present, to various degrees, with hepatosplenomegaly, tissue cholesteryl ester deposition, peripheral neuropathology, and a moderate increase in cardiovascular disease (CVD) risk (7). Despite the well-known effects of ABCA1 mutations on peripheral lipid and HDL metabolism, there are no reports of the impact of ABCA1 deficiency on brain HDL metabolism in humans.

The brain is the most cholesterol-rich organ in the body, containing over 25% of total body cholesterol in only 2% of total body weight (8). Dysfunctional brain lipid metabolism contributes to several neurodegenerative disorders, including Alzheimer's disease (AD) (9), Smith Lemli Opitz syndrome (10), and Neiman-Pick disease type II (11). Despite the importance of brain lipid metabolism for lifelong neuronal function, less is known about lipid and lipoprotein metabolism in the CNS compared with non-CNS tissues, primarily because CNS lipid metabolism is largely segregated from that of plasma. Under normal conditions, dietary cholesterol does not cross the blood-brain barrier (BBB), and all cholesterol required in the CNS is synthesized in situ (8). Unlike plasma, the CNS does not contain apoB-containing lipoproteins, including low-density lipoproteins (LDL), very low-density lipoproteins (VLDL), and chylomicrons (12). Instead, cholesterol and other lipids in

Abbreviations: ABCA1^{−/−}, ABCA1-deficient; AD, Alzheimer's disease; CNS, central nervous system; CSF, cerebrospinal fluid; EM, electron microscopy; FACS, fluorescence-activated cell sorting; GCM, glial-conditioned medium; KBr, potassium bromide; LDLR, LDL receptor; LDLR^{−/−}, LDLR deficient; LRP, LDL receptor-related protein; MW, molecular weight; RAP, receptor-associated protein; RCT, reverse cholesterol transport; RT, room temperature; TC, total cholesterol; WT, wild-type.
[1]To whom correspondence should be addressed.
   e-mail: cheryl@cmmt.ubc.ca

the CNS are transported on lipoprotein particles that resemble plasma HDL in size and density (12). ApoA-I is present in cerebrospinal fluid (CSF) at approximately 0.5% of its levels in plasma and may enter CSF by transfer across the BBB or via expression in choroid plexus epithelial cells (13–17). In contrast, full-length apoE does not cross the BBB (18), and the apoE in the CNS is synthesized and secreted by astrocytes and microglia (19, 20).

ApoE is a 299 amino acid protein that, in humans, is expressed as three genetic variants that differ by a single amino acid (21). These variants are apoE2 (cys112, cys158), apoE3 (cys112, arg158), and apoE4 (arg112, arg158) (21). ApoE genotype is the most established genetic risk factor for Alzheimer's disease in the general population (22). Carriers of the apoE4 allele display increased AD prevalence and an earlier age of onset in a gene dose-dependent manner (23), whereas inheritance of the apoE2 allele delays the age of onset and reduces AD prevalence (24). Although the precise mechanisms by which apoE contributes to AD pathogenesis is not entirely understood, apoE has a significant influence on the metabolism of Aβ peptides, which are the toxic species that accumulate as amyloid plaques in the neural parenchyma and cerebrovasculature of AD patients (9).

We and others have recently shown that the amount of lipids carried by apoE is an important determinant of Aβ metabolism in mice. Specifically, ABCA1$^{-/-}$ mice have poorly lipidated apoE that exacerbates the formation of amyloid plaques (25–27), whereas selective overexpression of ABCA1 by 6-fold or greater results in lipid-enriched apoE that inhibits amyloiodogenesis (28). Recently, ABCA1-mediated lipidation of apoE was shown to facilitate the proteolytic degradation of Aβ peptides by neprilysin and insulin-degrading enzyme (29). In addition to AD, the apoE4 genotype is associated with a worse prognosis after several types of acute neuronal insults (30). ApoE levels are presumably elevated in the injured brain to scavenge the vast amount of lipids released by degenerating neurons and myelin, which are later delivered to surviving neurons during reinnervation and synaptogenesis. These observations underscore the importance of understanding apoE HDL metabolism in the CNS for both acute and chronic neurological applications.

In plasma, HDL is not a single entity but, rather, exists as a complex and dynamic mixture of subclasses that differ in size as well as cholesterol, lipid, and protein composition (31, 32). These differences endow each HDL subclass with unique physiological properties with respect to receptor affinity, enzyme and protein association, cholesterol efflux capacity, size, and stability (31, 32). Subclass-specific properties are important aspects of RCT, where HDL must first accept lipids, become stabilized for transport through the bloodstream, and then offload its lipid cargo at target tissues (31, 32). ApoA-I, the key protein component of plasma HDL, is expressed in liver and intestine. Upon synthesis, ApoA-I is rapidly lipidated by ABCA1 to form nascent discoidal HDL particles, with liver ABCA1 generating approximately 70% of plasma HDL and intestinal ABCA1 contributing the remaining 30% (33, 34). These newly synthesized HDL particles have a discoidal shape, are com-

posed of two or three molecules of apoA-I, and form several distinct particle subtypes (1). For example, reconstituted nascent apoA-I HDL particles range from 7.8 to 17.0 nm in diameter and differ in their abilities to stimulate ABCA1-dependent cholesterol efflux and to bind and activate lecithin cholesterol acyltransferase (LCAT) (1). The LCAT reaction converts free unesterified cholesterol to cholesteryl ester (CE) during the maturation of immature nascent discoidal particles to mature spherical HDL (35), which is the preferred substrate for scavenger receptor class B type I (SR-BI)-mediated CE uptake by the liver and steroidogenic organs (36).

Compared with nascent apoA-I HDL particles in the periphery, less is known about the structure, function, and metabolism of nascent apoE HDL particles in the brain. Previous studies have shown that nascent apoE and apoJ are secreted as distinct particles from cultured primary astrocytes (37, 38). After 72 h of media conditioning, apoJ is found on particles approximately 8-11 nm in diameter with an irregular structure and contains approximately three parts protein and one part ethanolamine glycerophospholipids, whereas apoE forms nascent discoidal particles approximately 8, 11, and 14 nm in diameter, composed roughly of two parts protein, one part unesterified cholesterol, and one part phospholipids, with ethanolamine glycerophospholipids being approximately 3-fold more abundant than choline phospholipids (37, 38).

Similar to its role in plasma HDL biogenesis, ABCA1 has critical functions in the generation of apoE HDL in the CNS (39). Mice deficient in ABCA1 have an 80% loss of total apoE protein levels in brain tissue and exhibit reduced levels and abnormally small apoE lipoprotein particles in CSF (5, 6). Nascent apoE HDL particles secreted by ABCA1$^{-/-}$ glia are smaller and contain approximately 30% of the cholesterol found on wild-type (WT) particles (6). Intriguingly, ABCA1$^{-/-}$ glia secrete less apoE during the first 6-8 h of media conditioning (5), but by 72 h, total secreted apoE levels become equivalent between WT and ABCA1$^{-/-}$ cells (6). These observations suggest that glial apoE secretion also involves ABCA1-independent pathways. Here we show that ABCA1 facilitates the rapid secretion and lipidation of nascent apoE from primary glia to produce nascent HDL particles ranging from 7.5 to 17 nm in diameter. An ABCA1-independent pathway promotes the secretion of a poorly lipidated 8.1 nm apoE subspecies from both WT and ABCA1$^{-/-}$ glia, which is recycled primarily through the LDL receptor (LDLR).

MATERIALS AND METHODS

Animals

ABCA1$^{-/-}$ mice were obtained from Dr. Omar Francone (Pfizer Global Research and Development) and were on a DBA/1LacJ genetic background (40). LDLR$^{-/-}$ and apoE$^{-/-}$ mice, each on a C57Bl/6 background, as well as C57Bl/6 inbred mice, were obtained from Jackson Laboratories. Double LDLR/ABCA1$^{-/-}$ mice were generated by intercrossing single knockout lines followed by one backcross. Animals were maintained on a standard chow diet (PMI LabDiet 5010, containing 24% protein, 5.1% fat,

and 0.03% cholesterol). All procedures involving experimental animals were performed in accordance with approved protocols from the Canadian Council of Animal Care and the University of British Columbia Committee on Animal Care.

Primary glial culture

Primary mixed glia were prepared from postnatal day 0 to day 2 pups as described (5). Brains were removed and placed in ice-cold Hanks buffered salt solution (HBSS) adjusted to 6 g/l glucose and 10 mM 4-(2-hydroxyethyl)-1-piperazineethanesulfonic acid (HEPES) buffer. Meninges were removed, cortices and hippocampi were isolated, and tissues samples were minced with forceps and then homogenized by gentle trituration through a 5 ml pipette. Suspensions were centrifuged at 1,000 rpm for 4 min. The supernatant was discarded, and cells were resuspended in 3 ml of growth media (DMEM:F12 containing 10% fetal bovine serum, 2 mM L-glutamine, and 1% penicillin/streptomycin; Invitrogen). Each preparation from an individual pup was seeded into one T75 tissue culture flask with 13-15 ml growth media. Media were changed every 3-5 days until cells were fully confluent at approximately 14-20 days. Once confluent, cells were washed once with serum-free conditioning media and then incubated with serum-free conditioning media (1:1 DMEM:F12 with 0.2 mM penicillin and 0.05 mM streptomycin) for 72 h unless otherwise indicated. Glial-conditioned media (GCM) were harvested and centrifuged at 1,000 g for 3 min to remove any remaining cells, then concentrated 10× using Vivaspin 15 centrifugal concentrators with a molecular weight cutoff of 10,000 Da (Sartorius Mechatronics). GCM were stored at −20°C until analyzed. For cellular analysis, cells from one T75 flask were collected after incubation with 3 ml of 0.25% trypsin with EDTA for 5 min and centrifugation at 1,000 g for 3 min. Cell pellets were washed once with PBS. For protein analysis, cell pellets were lysed in 500 μl of radioimmunoprecipitation assay (RIPA) lysis buffer (20 mM Tris, 1% NP40, 5 mM EDTA, 50 mM NaCl, 10 mM Na pyrophosphate, 50 mM NaF, and complete protease inhibitor, pH 7.4). Cell lysates were sonicated at 30% output for 10 s. Overall protein concentration was determined by Lowry protein assay (Bio-Rad). Glial lysate samples were kept at −80°C until analyzed by 10% SDS-PAGE.

Fluorescence-activated cell sorting

Mixed glial cells were detached from a T75 culture flask with 0.25% trypsin for no more than 2 min, washed three times with ice-cold PBS, and triturated to a single-cell suspension in a fluorescence-activated cell sorting (FACS) buffer (2% FBS in 1× PBS). Cells were distributed into 96-well U-bottomed plates at approximately 1×10^6 cells per well and manipulated in the dark. Cells were incubated on ice for 30 min with 1:50 PE-anti-mouse CD11b antibody (#557397; BD Pharmingen). After two washes with FACS buffer, cells were fixed and permeabilized with BD Cytofix/Cytoperm solution (#554722; BD Biosciences) for 30 min on ice, washed twice with saponin-containing BD Perm/Wash buffer (#554723; BD Biosciences), and incubated with 1:25 Alexa Fluor 488-conjugated-anti-mouse GFAP antibody (#3655; Cell Signaling Technology) on ice for 30 min. After another two washes with saponin-containing buffer, the cells were resuspended in 2% PFA prior to FACS analyses. Cell fluorescence signals were determined by using a FACS Calibur (Becton Dickinson) equipped with highly sensitive blue (480 nm) and red (635 nm) lasers for quantitative analysis applications. Data were acquired and analyzed using CellQuestPro software (Becton Dickinson).

Conditioned media exchange

After 72 h, conditioned media were collected from a whole T75 flask of WT or ABCA1$^{-/-}$ primary glia and centrifuged at 1,000 g for 3 min to remove cellular debris. Half of the collected media was stored at −20°C, and the other half was transferred to a T75 flask of apoE$^{-/-}$ glia for another 48 h incubation. All collected media were concentrated 10× as above prior to analysis.

Electrophoresis and Western blotting

For native PAGE, GCM samples were mixed with nondenaturing loading dye to a final concentration of 0.04% bromophenol blue, 4.0% glycerol, and 100 mM Tris (pH 6.8) and resolved on 6% nondenaturing Tris-HCl polyacrylamide gels. For SDS-PAGE, media and cell samples were mixed with loading dye containing 2% SDS and 1% β-mercaptoethanol, incubated for 10 min at 90°C, and resolved on 10% Tris-HCl polyacrylamide gels. Proteins were transferred onto polyvinylidene difluoride (PVDF; Millipore) membranes at 24 V overnight at 4°C. After blocking with 5% nonfat milk in PBS for 1 h, membranes were probed with 1:1000 goat-anti-murine apoE (Santa Cruz Biotechnology and Chemicon), 1:2500 goat-anti-human apoE (Biodesign), 1:1000 rabbit-anti-human apoJ (Signet), 1:1000 monoclonal anti-ABCA1 (a gift from Dr. Michael Hayden), 1:1000 goat-anti-LDLR (R and D Systems), and 1:2000 rabbit-anti-LRP (a gift from Dr. Joachim Herz) overnight at 4°C. The Biodesign antibody to human apoE cross-reacts with murine apoE. Membranes were washed with 2× PBS-T (2× PBS with 0.05% Tween-20) four times for 8 min each and then incubated for 1 h with 1:1000 horseradish peroxidase (HRP)-labeled anti-goat secondary antibody (Santa Cruz Biotechnology). Results were visualized using chemiluminescence (Amersham). Particle diameters on native gels were determined by comparison with a native high molecular weight marker standard (Amersham). Protein molecular weights on denaturing gels were determined by comparison with the kaleidoscope molecular weight marker standard (Bio-Rad).

Potassium bromide gradient ultracentrifugation

An amount of 3 ml of CGM, conditioned for 72 h and concentrated 5×, was adjusted to a density of 1.25 g/ml with potassium bromide (KBr) salt and overlaid with 2.0 ml of 1.225 g/ml, 4.0 ml of 1.100 g/ml, and 3.0 ml of 1.006 g/ml KBr solutions. Gradients were centrifuged for 21 h 15 min at 40,000 rpm at 20°C in a SW41 rotor (Beckman). Four fractions were collected from the top of the gradient: fraction 1 = 4 ml (1.060 g/ml), fraction 2 = 3 ml (1.122 g/ml), fraction 3 = 3 ml (1.195 g/ml), and fraction 4 = 2 ml (1.252 g/ml). Fractions were dialyzed against PBS at 4°C overnight, then concentrated 10× using Centriprep YM-10 concentrators with molecular weight cutoff of 10,000 Da (Millipore) and analyzed by 6% native PAGE and 10% SDS-PAGE. Total cholesterol (TC) content of fractions was measured using commercially available enzymatic kits (Invitrogen) following the manufacturer's instructions.

Electron microscopy

Three hundred fifty microliters of concentrated GCM was dialyzed against electron microscopy (EM) dialysis buffer (0.125 M ammonium acetate, 2.6 mM ammonium carbonate, and 0.26 mM EDTA) overnight at 4°C. Then, 2 μl of each sample was mixed with 2 μl of 2% sodium phosphotungstate and incubated for 1 min. Next, 5 μl of the stained sample was loaded onto formvar- and carbon-coated copper grids (Canemco). Excess solution was immediately absorbed with filter paper, and the samples were air dried on the grid. Particles were imaged on a Hitachi H7600 transmission electron microscope using an AMT Advantage HR Digital CCD camera.

Oil Red O staining

Glial cells were seeded in poly-D-lysine-coated 12-well plates at 300,000 cells/well. After 24 h in DMEM containing 10% fetal FBS, cells were air dried, fixed in neutral-buffered formalin, and stained with Oil Red O. Nuclei were counterstained with

hematoxylin. Cells were photographed on a Zeiss Axioplan 2 microscope using a CCD camera equipped with AxioVision Rel. 4.6 (Carl Zeiss, Inc.) imaging software.

RAP purification

A single colony of BL21 *E. coli* containing pGEX-KG-RAP (a gift from Dr. Joachim Herz) was inoculated into 10 ml of 2× YT media and cultured overnight at 37°C, with shaking at 220 rpm. The 10 ml culture was diluted with 1 l of 2× YT media and cultured using the same conditions until OD600 = 0.8-1.0. Expression of GST-RAP was induced by adding 0.5 M isopropyl-beta-d-thio-galactopyranoside (IPTG) to a final concentration of 0.2 mM for 1 h. Cells were harvested by centrifugation at 5,000 rpm for 10 min at 4°C, then washed with 1× PBS and centrifuged as before. Cells were resuspended in 60 ml of lysis buffer (1× PBS, protease inhibitor, 10% glycerol, and 1% Triton X-100 and fresh lysozyme powder [100 mg/ml]) and incubated on ice for 15 min. Cells were sonicated three times for 15 s at 20% amplitude and cleared by centrifugation at 12,000 rpm for 15 min. The supernatant was then incubated for 3 h at room temperature (RT) with 1 ml glutathione sepharose beads (previously equilibrated with 1× PBS) for every liter of culture. Beads were centrifuged at 2,000 rpm, and then washed three times with 1× PBS. Beads were then equilibrated with 1× precision protease buffer (50 mM Tris-Cl pH 7.0, 150 mM NaCl, 1 mM EDTA, and 1 mM DTT) before incubation with protease solution (30 units in 1 ml of protease buffer per 1 l culture) at RT overnight. Eluate was collected, and another 1 ml of fresh protease buffer was added to the beads and incubated at RT overnight. Eluate samples were pooled and concentrated 10× using Centriprep YM-10 concentrators (Millipore), and then analyzed on a 10% SDS-PAGE gel stained with Coomassie Blue for quantification.

RAP inhibition of apoE uptake

Wild-type and ABCA1$^{-/-}$ glia were reseeded into 12-well plates at a density of 400,000-500,000 cells/well in 1 ml of maintenance media (DMEM:F12 containing 10% FBS, 2 mM L-glutamine, and 1% penicillin/streptomycin). After 48 h, cells were treated with either 500 μl of serum-free conditioning media (DMEM:F12) or serum-free conditioning media containing 1 μM BSA, 70 nM RAP, or 1 μM RAP for 72 h. Conditioned media were collected, and cells were harvested using 100 μl of RIPA lysis buffer followed by Western blot analysis on nondenaturing or denaturing gels as described above.

ApoE ELISA

The 96-well ELISA plates (Costar cat. #3590; Fisher) were coated with 3.13 ng/well WUE4 apoE antibody (a kind gift from Dr. David Holtzman) at 4°C overnight, then washed five times with PBS-0.025% Tween (pH 7.4), blocked with 1% nonfat dry milk in PBS (pH 7.4) for 1 h, and then washed as above. Standards or samples were diluted with dilution buffer (DB, 0.5% BSA and 0.025% Tween 20 in PBS, pH 7.4) and heated at 52°C for 3 h. Wells were loaded with 100 μl of sample in duplicate and 100 μl of apoE standards in triplicate, incubated in a humid chamber for 24 h at 4°C, then aspirated and washed as before. Next 100 μl per well of Calbiochem anti-apoE (1:12,000) in DB was added and incubated for 90 min at 37°C. After washing, 100 μl per well of biotinylated anti-goat IgG (1:160,000; Vector) in DB was added and incubated for 90 min at 37°C. Streptavidin-poly-HRP antibody (1:4000; Pierce) was then added and incubated at RT for 90 min. Color was developed by adding 100 μl/well Sigma ELISA TMB and stopped immediately by adding 100 μl of 1M HCL. Plates were read at 450 nm absorbance.

Cholesterol and phospholipid measurement

Total cholesterol measurements of GCM samples were performed using the fluorogenic Amplex Red Cholesterol Assay Kit (Invitrogen) following the manufacture's protocol. To measure total cholesterol and phospholipids levels in cells, cellular lipids were extracted using a modified Bligh and Dyer method. Briefly, a cell suspension was added to 1:2 (v/v) chloroform:methanol, vortexed for 30 s, and centrifuged at 1,000 *g* for 5 min. The supernatant was then transferred to 1:1 (v/v) chloroform:0.9% NaCl solution. After another centrifugation at 1,000 *g* for 5 min, the chloroform phase was transferred to new glass tube and dried under nitrogen. After the lipid pellet was dissolved in 2% Triton-X 100, cellular total cholesterol and phospholipid content was measured by Wako kits following the manufacture's protocols (#439-35801 for Cholesterol E kit and #433-36201 for Phospholipids C kit; Wako).

Preparation of recombinant apoA-I

Human apoA-I was expressed in bacteria as previously described (41). The protein was expressed in *E. coli* strain BL21 (DE-3) pLysS and cultured in NZ amine, Casamino acids, Yeast extract, Mgso4 (NZCYM) media containing 50 μg/ml ampicillin. Expressed proteins were purified via Hi-Trap nickel chelating columns (GE Biosciences) as described (41). Protein purity (>95%) was confirmed by SDS-PAGE.

Statistical analysis

Data are shown as mean ± standard error. One-way ANOVA with a Tukey's multiple comparison post test or two-tailed unpaired Student's *t*-test were used for statistical analysis. For *t*-test analyses, Welch's correction for unequal variances was applied when variances were significantly different between groups. All statistical analyses were performed using GraphPad Prism (version 5.0; GraphPad Software for Science, Inc.).

RESULTS

Nascent apoE particle subspecies are secreted from WT and ABCA1$^{-/-}$ glia in a distinct temporal pattern

Previous studies have suggested that ABCA1$^{-/-}$ glia secrete less apoE within the first 6-8 h of conditioning compared with WT glia but that total apoE levels become equivalent after 72 h (5, 6). To further delineate the dynamic nature of glial apoE secretion, we characterized the electrophoretic pattern of apoE subspecies secreted from mixed primary WT and ABCA1$^{-/-}$ glia after 6, 24, 48, and 72 h of conditioning. FACS analysis showed that WT and ABCA1$^{-/-}$ cultures contained comparable amounts of GFAP-positive astrocytes and CD11b-positive microglia (astrocytes: WT = 80.71 ± 4.73%, N = 5, ABCA1 = 84.07 ± 3.39%, N = 5, *P* > 0.05; microglia: WT = 2.68 ± 1.17%, N = 5, ABCA1 = 3.25 ± 1.95%, N = 5, *P* > 0.05). Native PAGE analysis showed that WT glia secreted several apoE nascent particles ranging in diameter from approximately 7.5 to 17 nm, including an 8.1 nm species that required at least 48 h of conditioning to become detectable in WT glial-conditioned media (**Fig. 1**). ABCA1$^{-/-}$ glia secreted only the 8.1 nm particle. SDS-PAGE analysis confirmed that ABCA1$^{-/-}$ glia secreted less total apoE during the first 6 h of conditioning.

The 8.1 nm particle secreted from WT and ABCA1$^{-/-}$ glia is a lipid-poor and structurally distinct species

Wahrle et al. previously reported that the total cholesterol content of conditioned media from ABCA1$^{-/-}$ astrocytes
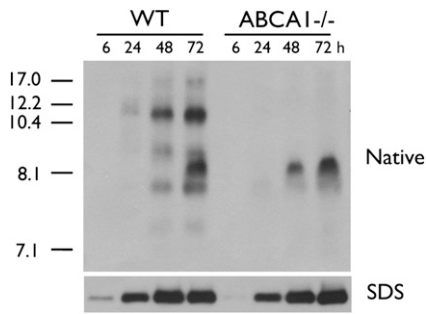
Fig. 1. Glial apoE is secreted as distinct nascent subspecies. WT and ABCA1$^{-/-}$ primary mixed glia were cultured to confluency and then conditioned in serum-free media for indicated time points. Media were collected, concentrated 10-fold, and analyzed by 6% native PAGE followed by immunoblotting for apoE. Stokes diameter of standards are listed on the left.

is reduced by 70% compared with WT controls (6), indicating that the 8.1 nm species is lipid poor. To confirm this observation, we quantified the TC and total apoE levels in 72 h GCM by enzymatic assay and ELISA, respectively, and observed a 79% decrease in TC (WT: 72.3 μg TC/μg apoE; ABCA1$^{-/-}$: 15.1 μg TC/μg apoE, $P < 0.001$), consistent with Wahrle's earlier observation (6). To determine if there were differences in lipidation of individual glial-derived nascent apoE subspecies, we next performed KBr gradient ultracentrifugation to separate the particles by buoyant density. Western blot analysis of KBr fractions showed that all particles secreted by WT glia except the 8.1 nm species were recovered in fraction 2 (1.1-1.2 g/ml) (**Fig. 2A**). In contrast, the 8.1 nm particle from both WT and ABCA1$^{-/-}$ glia was recovered in fraction 4 (>1.25 g/ml) (Fig. 2A). ApoJ, a protein-dense lipoprotein secreted from glia, was also recovered in fraction 4 from both WT and ABCA1$^{-/-}$ media (Fig. 2A). These observations indicate that the 8.1 nm particle, detectable in WT GCM by 48-72 h, is equivalent to the 8.1 poorly lipidated species that is the sole apoE particle found in ABCA1$^{-/-}$ GCM. Negative-staining EM of conditioned media from WT and ABCA1$^{-/-}$ glia revealed that the rouleaux characteristic of discoidal HDL particles was observed in WT but not ABCA1$^{-/-}$ samples, suggesting that the 8.1 nm particle is nondiscoidal and structurally incapable of forming these distinctive stacks (Fig. 2B).

Lipidation of the 8.1 nm apoE particle by ABCA1 restores apoE subspecies distribution to resemble the WT pattern

Because the 8.1 nm apoE particle was a structurally distinct lipid-poor HDL particle relative to the other nascent apoE HDL particles secreted by WT glia, we next queried whether it was capable of accepting lipids from ABCA1. Media from WT and ABCA1$^{-/-}$ glia were conditioned for 72 h and then added to apoE$^{-/-}$ glia for an additional 48 h to allow the donor particles to be lipidated by ABCA1 expressed in the recipient cells. Donor apoE particles secreted from both WT and ABCA1$^{-/-}$ glia gave rise to a nearly identical pattern of apoE particles after incubation with ABCA1-expressing apoE$^{-/-}$ glia (**Fig. 3**). The only particle that ABCA1$^{-/-}$ donor media failed to generate was a large
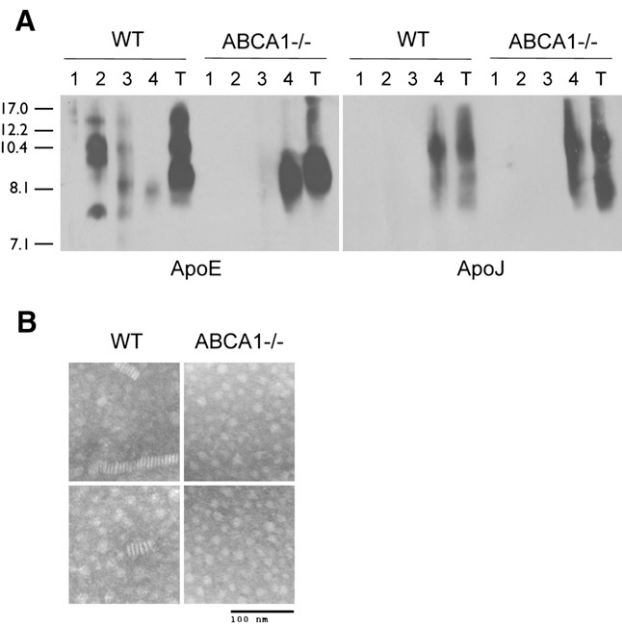
Fig. 2. The 8.1 nm apoE particle is protein dense and incapable of forming rouleaux. A: Confluent WT and ABCA1$^{-/-}$ primary mixed glia were conditioned in serum-free media for 72 h. Media were collected, concentrated 10-fold, and analyzed by KBr ultracentrifugation. Samples were separated into four fractions: fraction 1 = 1.060 g/ml, fraction 2 = 1.122 g/ml, fraction 3 = 1.195 g/ml, and fraction 4 = 1.252 g/ml. Fractions were dialyzed, concentrated, and analyzed by 6% native PAGE followed by immunoblotting to apoE and apoJ relative to unfractionated total (T) conditioned media. Stokes diameter of standards are listed on the left. B: Negative-stain EM of media conditioned from WT and ABCA1$^{-/-}$ primary mixed glia for 72 h, showing two representative images for each genotype and magnification (bar).

species at approximately 17 nm. These observations demonstrate that, despite its structurally distinct nature, the 8.1 nm apoE particles are not impaired in their ability to accept lipids from ABCA1.
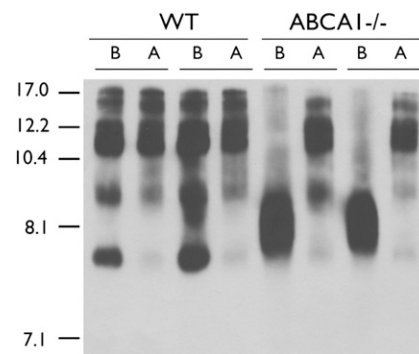
Fig. 3. The 8.1 nm apoE particle is an efficient lipid acceptor for ABCA1. Confluent WT and ABCA1$^{-/-}$ primary mixed glia were conditioned in serum-free media for 72 h. Media were collected and added to confluent primary apoE$^{-/-}$ mixed glia for an additional 48 h, then analyzed by 6% native PAGE followed by immunoblotting to apoE. The gel shows media samples from two independent animals per genotype before (B) and after (A) exposure to apoE$^{-/-}$ glia. Stokes diameter of standards are listed on the left.

ABCA1 deficiency reduces LDLR levels in cultured glia

We have previously shown that ABCA1-deficient glia accumulate lipids under standard culture conditions (5). We confirmed and extended these observations by first staining for neutral lipids using Oil-Red-O in WT, ABCA1$^{-/-}$, and LDLR$^{-/-}$ glia. As expected, we observed minimal lipid droplets in WT glia, abundant lipid droplets in ABCA1$^{-/-}$ glia, and no lipid accumulation in LDLR$^{-/-}$ glia (**Fig. 4A**). Because cellular lipid accumulation in ABCA1$^{-/-}$ cells is expected to activate sterol-regulatory element binding protein 2 (SREBP2) that leads to negative feedback regulation of LDLR but not LRP expression, we next quantified LDLR and LRP levels by Western blot. As expected from the presence of lipid accumulation, ABCA1$^{-/-}$ cells exhibited a 75% reduction in LDLR protein levels compared with WT glia (P < 0.0001, Fig. 4B) but no significant change in LRP levels compared with WT glia. The selective reduction in LDLR levels in ABCA1$^{-/-}$ glia indicates that the ratio of LRP:LDLR is likely lower in ABCA1$^{-/-}$ relative to WT glia under the culture conditions employed. There were no significant differences in cellular apoE levels among WT, ABCA1$^{-/-}$, and LDLR$^{-/-}$ glia (Fig. 4B).

Inhibition of apoE receptor activity preferentially reduces secretion of small apoE particles from glia

In several cell types, apoE is recycled through apoE receptor-mediated endocytosis and resecretion (42–45). To determine if apoE recycling also occurs in primary glia, we first examined the distribution pattern of secreted apoE particles over time in WT and LDLR$^{-/-}$ glia. Appearance of apoE particles in LDLR$^{-/-}$ GCM was delayed relative to WT GCM (**Fig. 5**). Furthermore, the 8.1 nm apoE particle was barely detectable even after 96 h of conditioning (Fig. 5). Selective deletion of the LDLR did not alter cellular TC content in LDLR$^{-/-}$ compared with WT glia (WT = 27.09 ± 2.232 ng TC/ng protein, N = 4, LDLR$^{-/-}$ = 25.78 ± 1.111 ng TC/ng protein, N = 5, P = 0.592). These observations are consistent with a role for LDLR in apoE recycling and with the effect of loss of LDLR activity on the 8.1 nm particle.

To further differentiate the roles of glial LRP and LDLR on secretion of apoE subspecies, we also used recombinant RAP, prepared as a GST-fusion protein, to block the activity of apoE receptors. RAP inhibits LRP at 70 nM and both LRP and LDLR at 1 μM (46). The levels and pattern of secreted apoE subspecies were not altered when WT, ABCA1$^{-/-}$, and LDLR$^{-/-}$ glia were incubated with 1 μM
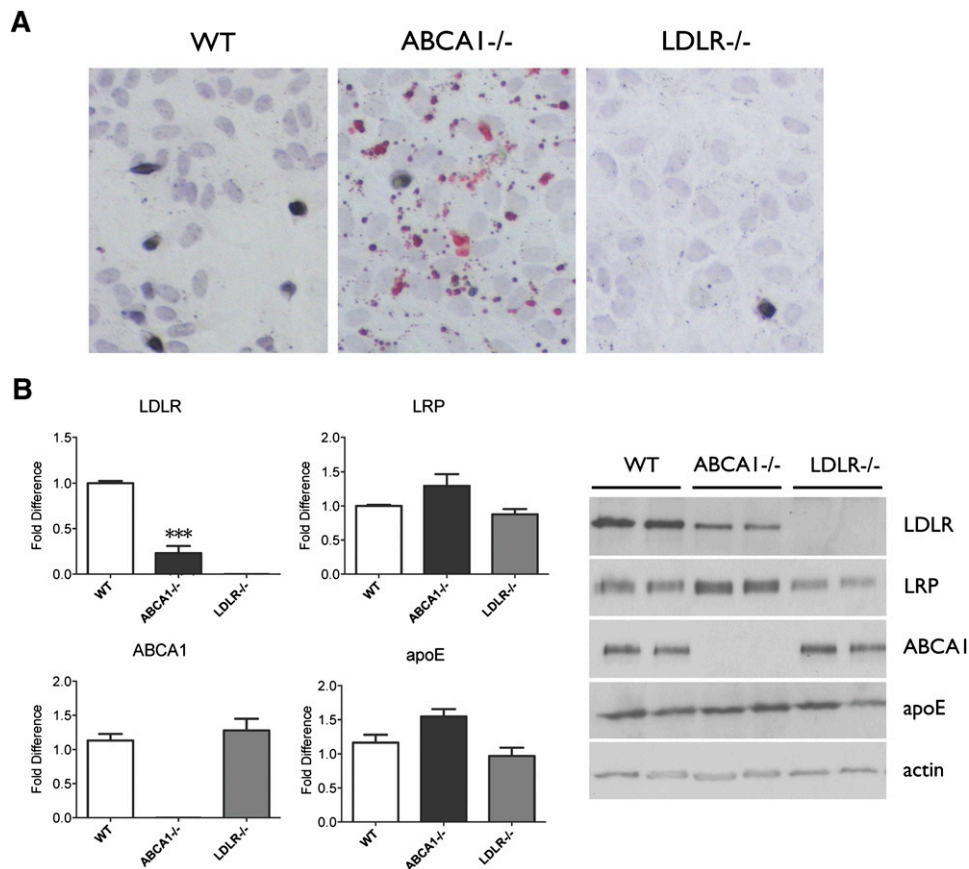
Fig. 4. ABCA1$^{-/-}$ glia accumulate lipids and have reduced LDLR levels. A: Oil-Red-O staining of neutral lipids in WT, ABCA1$^{-/-}$, and LDLR$^{-/-}$ primary mixed glia at confluency. B: Quantification of cellular LDLR and LRP expression in WT, ABCA1$^{-/-}$, and LDLR$^{-/-}$ primary mixed glia by Western blot. Actin was used as a loading control. Data represent means and standard error of N = 6-9 independent cultures. ***P < 0.001 using one-way ANOVA with Tukey's multiple comparison post test.
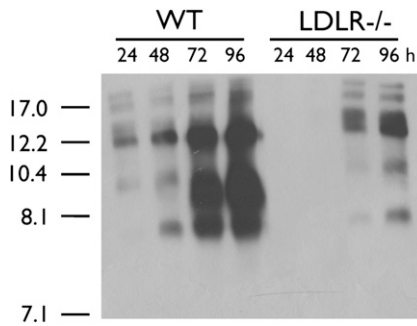
Fig. 5. LDLR deficiency leads to a selective loss in the 8.1 nm apoE particle. WT and LDLR$^{-/-}$ primary mixed glia were cultured to confluency and then conditioned in serum-free media for indicated time points. Media were collected, concentrated 10-fold, and analyzed by 6% native PAGE followed by immunoblotting for apoE. Stokes diameter of standards are listed on the left.

BSA as a negative control or with 70 nM RAP, suggesting that LRP does not play a major role in regulating the levels of secreted apoE (**Fig. 6A**, left panel). In contrast, treatment of WT and LDLR$^{-/-}$ glia with 1 μM RAP reduced the total level of secreted apoE and preferentially inhibited the secretion of the smaller apoE subspecies, leaving only the larger 12-17 nm particles evident in GCM (Fig. 6A, left panel). Although treatment of ABCA1$^{-/-}$ glia with 70 nM RAP had no impact on secreted apoE levels, treatment with 1 μM RAP blocked the secretion of the 8.1 nm apoE species, virtually eliminating the secretion of apoE (Fig. 6A). That functional inhibition of apoE receptors reduces secreted apoE is consistent with the hypothesis that apoE recycling, primarily via LDLR, contributes to the steady-state apoE levels in GCM. Furthermore, by inhibiting apoE uptake, RAP-mediated inhibition of glial apoE receptors may prolong the extracellular half-life of secreted apoE and increase its availability to ABCA1, thus generating larger particles in cells that are capable of cholesterol efflux.

To specifically delineate the contribution of LDLR to apoE recycling in glia, we generated double knockout (DKO) ABCA1$^{-/-}$/LDLR$^{-/-}$ mice and evaluated apoE secretion from primary mixed glia. Densitometric analysis of apoE levels in GCM by SDS-PAGE suggested at least a 70% reduction in total apoE levels in 72 h DKO GCM (WT: 7.33 ± 4.17 optical units, ABCA1$^{-/-}$: 7.21 ± 4.23 optical units, DKO: 2.12 ± 1.01 optical units) (Fig. 6B). More accurate quantitation of total apoE levels by ELISA showed that apoE secretion was reduced by approximately 93% in 72 h DKO GCM (WT: 123.5 ± 1.66 ng/ml, ABCA1$^{-/-}$: 123.9 ± 10.83 ng/ml, DKO: 8.72 ± 1.13 ng/ml) (Fig. 6C). Because LDLR levels in ABCA1$^{-/-}$ glia are only approximately 25% of WT levels under the culture conditions employed here (Fig. 6B, C), these observations clearly define a major role for the LDLR in ABCA1-independent apoE recycling/secretion, as LRP cannot compensate efficiently for LDLR with respect to apoE recycling.
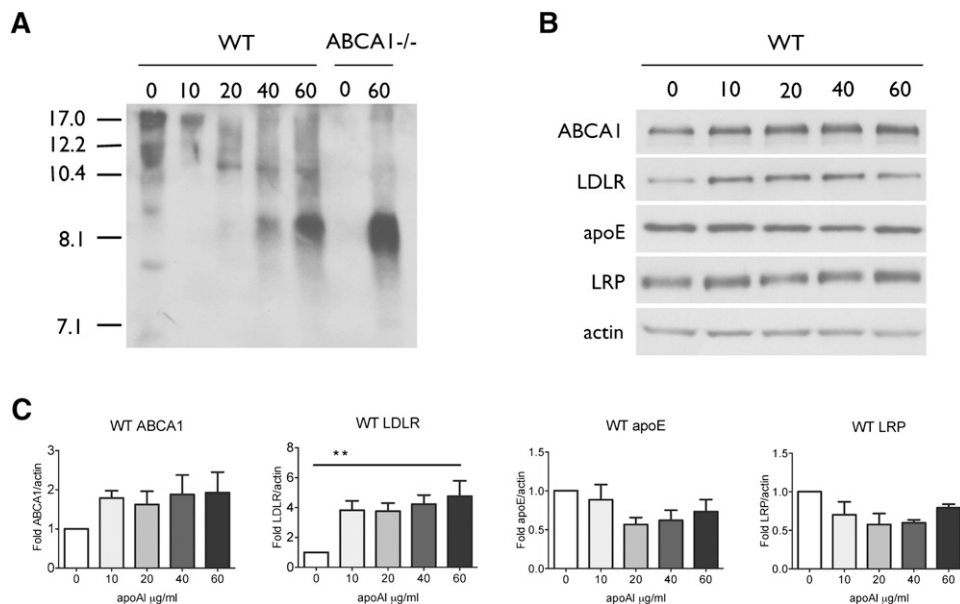
ApoA-I stimulates glial apoE recycling and lipidation in primary glia

ApoA-I and HDL have been reported to stimulate apoE recycling in a wide variety of cell types, including Chinese
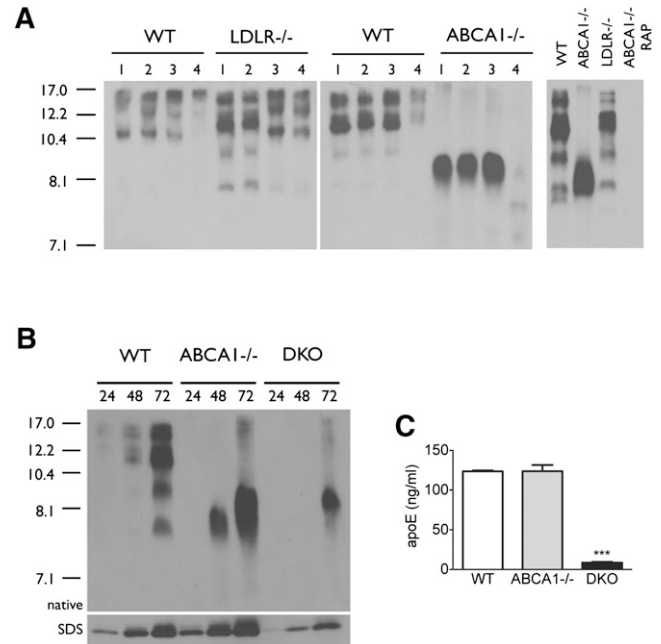
Fig. 6. Secretion of the 8.1 nm apoE particle involves LDLR function. A: Confluent WT, LDLR$^{-/-}$, and ABCA1$^{-/-}$ primary mixed glia were treated with serum-free media containing no additives (1), 1 μM BSA (2), 70 nM RAP (3), or 1 μM RAP (4) for 72 h (left panel). Confluent WT and LDLR$^{-/-}$ primary mixed glia were conditioned for 72 h in the absence of RAP, and primary ABCA1$^{-/-}$ glia were conditioned for 72 with and without 1 μM RAP as indicated (right panel). Media were collected and analyzed by native PAGE followed by immunoblotting to apoE. B: Confluent WT, ABCA1$^{-/-}$, and ABCA1/LDLR$^{-/-}$ primary mixed glia were conditioned in serum-free media for 72 h. Media were collected at the indicated time points and analyzed by native and SDS-PAGE followed by immunoblotting to apoE. Stokes diameter of standards are listed on the left. C: Quantitation of apoE levels in media from WT, ABCA1$^{-/-}$, and ABCA1/LDLR$^{-/-}$ conditioned media by ELISA. Data represent means and standard error from two independent cultures per genotype using one-way ANOVA with Tukey's multiple comparison post test.

hamster ovary (CHO) cells, fibroblasts, hepatocytes, macrophages, adipocytes, and neuronal cells (42, 47–55). In macrophages, apoA-I-mediated stimulation of apoE secretion is independent of ABCA1 (56). To determine whether apoA-I stimulates apoE secretion from primary glia, we treated mixed glial cultures with recombinant human apoA-I at doses ranging from 10 to 60 μg/ml for 48 h. Conditioned media showed a clear dose-dependent increase in 8.1 nm apoE particles (**Fig. 7A**), supporting our hypothesis that this species represents recycled apoE that, in WT cells, has not yet been lipidated by ABCA1. The decreased signal of larger particles (>10 nm) in WT media suggests that secreted apoE might be driven more toward the recycling pathway rather than lipidation in the presence of apoA-I. ApoA-I treatment of WT glia also led to a significant increase in cellular LDLR levels, further supporting a role for LDLR in glial apoE recycling (Fig. 7B, C). It also led to a trend toward increased ABCA1 and decreased cellular apoE levels (Fig. 7B, C). Cellular LRP levels were not significantly affected by apoA-I treatment (Fig. 7B, C).

Fig. 7. ApoA-I stimulates apoE recycling from glia. A: WT primary glia were conditioned for 48 h in the absence or presence of the indicated concentrations of recombinant human apoA-I. Samples were concentrated 10× and analyzed by nondenaturing PAGE and immunodetection for apoE. B: Cell lysates of primary glia treated with the indicated concentrations of recombinant human apoA-I were separated by SDS-PAGE and immunodetected for ABCA1, LDLR, apoE, LRP, and actin as a loading control. C: Quantitation of cellular ABCA1, LDLR, apoE, and LRP levels in WT glia-treated apoA-I. Data represent means and standard error from three independent experiments using one-way ANOVA with Tukey's multiple comparison post test.

DISCUSSION

ApoE is at the hub of CNS HDL metabolism and the most important genetic risk factor for sporadic AD. Several lines of evidence suggest that aberrant CNS lipid metabolism may contribute to AD pathogenesis (9). Of particular interest is the discovery that ABCA1-mediated lipidation of apoE facilitates the degradation and clearance of Aβ peptides, potentially offering a mechanism for novel therapeutic strategies for AD. Developing such therapeutic approaches will likely require a deeper understanding of the metabolism of brain HDL particles than presently exists. It is likely that CNS apoE HDL comprise distinct specialized lipoprotein subspecies, similar to complexity of plasma HDL, which are a heterogeneous mixture of subclasses with both structural and functional differences (1, 32). In this article, we provided evidence for structural and physiological differences in nascent apoE-derived lipoproteins secreted from glia.

ApoE appears in glial-conditioned media as a variety of nascent particles ranging from 7.5 to 17 nm in diameter, a larger size range than previously reported (6, 19, 37, 38). Most of the earlier studies allowed media to condition for extended periods of time (i.e., 72 h) to allow apoE to accumulate to sufficient levels for detection. We analyzed secreted apoE subspecies from 6 to 72 h, and we demonstrated that particle diameters are modulated over this time course, suggesting that there may be extensive remodeling of apoE species that could occur through direct interaction among secreted particles in the media, through interactions at the cellular membrane, or via apoE uptake and recycling mediated by apoE receptors.

In particular, both WT and ABCA1$^{-/-}$ glia secrete an 8.1 nm apoE particle that is structurally and functionally distinct from the other species secreted from WT cells. We hypothesized that this particle is recycled apoE that emerges from the cell in a lipid-poor state independent of ABCA1 and is rapidly lipidated if cells express functional ABCA1. Supporting this hypothesis are the following observations. First, the 8.1 nm particle is lipid poor. The 8.1 nm particle is the sole species secreted from ABCA1$^{-/-}$ glia, and previous studies using gel filtration chromatography and media TC measurements demonstrated its paucity of lipids (6). Here we showed that this 8.1 nm particle is also detectable in WT GCM and that it resolves in a lipid-poor fraction by KBr density gradient ultracentrifugation when isolated from either WT or ABCA1$^{-/-}$ glia. Second, it is structurally distinct from the other apoE species. Negative-staining EM indicates that it is unable to form rouleaux characteristic of discoidal lipoprotein particles, consistent with the "figure-8" structure for similarly sized peripheral apoA-I-containing HDL particles predicted by Catte et al. (57) and observed by Cavigiolio et al. (32) and Zhang et al. (58). Nevertheless, it is not a dead-end particle with respect to RCT, as conditioned media swap experiments demonstrated that it is fully capable of accepting lipids effluxed by ABCA1 to form the full repertoire of particles normally observed in WT GCM. Third, blocking apoE receptor function by RAP inhibits the appearance of the 8.1 nm particle from ABCA1$^{-/-}$ glia, suggesting that it

may arise through an ABCA1-independent recycling pathway dependent on apoE receptors.

Our data suggests that apoE may be recycled primarily through LDLR in glial cultures. In ABCA1$^{-/-}$ glia, accumulation of lipid droplets triggers feedback regulation that suppresses LDLR expression to approximately 25% of normal levels but does not significantly impair apoE secretion after extended conditioning periods. However, decreasing LDLR levels from 25% to zero by selectively deleting LDLR in ABCA1$^{-/-}$ glia greatly impeded apoE secretion to approximately 10% of WT levels. Further, RAP added to levels that would reduce only LRP function did not have an effect on apoE secretion from WT or ABCA1$^{-/-}$ glia, but addition of 1 μM RAP to inhibit both LRP and LDLR markedly impaired apoE secretion from ABCA1$^{-/-}$ cells. These findings suggest that even though LRP is abundantly expressed in ABCA1$^{-/-}$ glia, it does not compensate well for LDLR in glial apoE recycling.

Intriguingly, lipid-poor apoE particles secreted from human embryonic kidney (HEK) cells were found to self-assemble into a high molecular weight (MW) mass that bound more avidly to LRP than LDLR (59). This may be due to the size of these high MW species, as small apoE-containing triglyceride-rich emulsions have impaired LDLR-dependent clearance in rats but emulsions of large particles are cleared independently of LDLR (60). Experiments in primary hepatocytes showed that apoE reconstituted into VLDL particles was recycled normally in LDLR$^{-/-}$ cells even though uptake was reduced by 50% (61). Similar experiments using RAP$^{-/-}$ hepatocytes, which had a 75% reduction in LRP levels, also indicated that apoE was recycled normally (61). These results suggest that, in hepatocytes, efficient apoE recycling can be mediated by either LDLR or LRP, at least when apoE is reconstituted in VLDL particles. Whether recycling of small nascent apoE-only particles may have a preference for LDLR or LRP in hepatocytes is not yet known. Understanding the differences between high MW HEK-derived apoE particles, reconstituted apoE-VLDL particles, and nascent glial-derived apoE particles may offer insight into the factors that govern apoE receptor preference.

Taken together, our results define two pathways that regulate the steady-state levels of glial-derived secreted apoE. One pathway requires ABCA1 and leads to the accumulation of several lipidated discoidal nascent apoE particles from 7 to 17 nm in diameter. The other pathway requires functional apoE receptors, primarily LDLR, and selectively regulates the secretion of a distinct 8.1 nm poorly lipidated apoE species, which is likely resecreted following LDLR-mediated apoE uptake. Secretion of this particle does not require ABCA1, but when ABCA1 is present, the particle is rapidly lipidated and difficult to detect in WT GCM.

Previous studies suggest that 60–80% of internalized apoE may be recycled (42–45) and directed to HDL particles (62) in non-CNS tissues. For example, triglyceride-rich lipoproteins taken up by hepatocytes via apoE receptors are differentially sorted after endocytosis. Core lipids and apoB are targeted to lysosomes, whereas the majority of apoE is delivered to recycling endosomes where it

can be mobilized by apoA-I or HDL to be recycled back to the plasma membrane, followed by resecretion and relipidation of apoE to form apoE HDL (42, 49). In macrophages, FPLC analysis demonstrated that recycled apoE is present on small HDL, suggesting that it either exits the cell in a lipidated form or is swiftly lipidated by ABCA1 (50). The results presented in this article suggest that glia also share these pathways.

HDL or purified apoA-I stimulates the release of internalized apoE from CHO cells, hepatocytes, fibroblasts, adipocytes, macrophages, and neuronal cells (42, 47–55). The mechanism by which apoA-I or HDL stimulates apoE recycling is not yet clear. In hepatoma cells, HDL-derived apoA-I colocalizes with apoE in EEA-1 positive early endosomes (48). ABCA1 colocalizes with internalized apoA-I in macrophages (63) and modulates late endocytic trafficking (64). These observations suggest that ABCA1, apoA-I, and apoE may have intracellular interactions that promote apoE recycling. Much remains to be learned, however, as internalized apoA-I is apparently not resecreted efficiently and has been reported to contribute to only 1.4% of total HDL production (65). Further, because secreted apoE levels are equivalent between WT and ABCA1$^{-/-}$ glia after extended conditioning times (6), ABCA1 is clearly not required for apoE recycling in glia. These observations parallel the previous observation that apoA-I stimulates apoE secretion from macrophages independent of ABCA1 (56).

Because most of the apoA-I in the CNS is found in CSF and is not synthesized by glia (16, 17, 19), the relevance of apoA-I-mediated stimulation of apoE recycling in the CNS is not immediately evident. However, several recent studies suggest that apoA-I affects CNS function and impacts the pathogenesis of AD. For example, although deletion of apoA-I alone has no effect on memory, apoA-I$^{-/-}$ mice crossed with the APP/PS1 mouse model of AD exhibited increased inflammation and impaired spatial learning and memory retention compared with APP/PS1 controls (66). Conversely, 2-fold overexpression of apoA-I protected APP/PS1 mice from inflammation and age-associated learning and memory deficits (67). These changes were independent of APP processing, did not influence soluble or insoluble Aβ$_{40}$ or Aβ$_{42}$ levels or amyloid plaque burden (66–68), and did not affect the levels of brain apoE (66, 68), ABCA1 (66), or cholesterol content (66, 67). However, APP/PS1 apoA-I$^{-/-}$ mice showed a 10-fold increase in insoluble Aβ$_{40}$ and a 1.5-fold increase in Aβ$_{42}$ in cortical and hippocampal blood vessels, indicating that these mice had significantly increased cerebral amyloid angiopathy (CAA) (66). In contrast, levels of CAA were decreased by 44% in APP/PS1 mice overexpressing apoA-I (67). These studies demonstrate that, although apoA-I is not a major apolipoprotein in brain parenchyma, it nevertheless can influence inflammation, cognitive function, and Aβ metabolism in the cerebral vasculature. Whether brain delivery of apoA-I can be used to stimulate apoE recycling and promote brain RCT now becomes an important question to pursue.

The relevance of this question is highlighted by recent findings on the importance of apoE genotype on recycling

and brain physiology. ApoE4 is impaired in HDL-induced recycling of triglyceride-rich lipoproteins (69). Furthermore, the low pH of lysosomes may preferentially affect the molten globule structure of apoE4 and retard its release into the recycling pathway (70–73). ApoE3 binds HDL more readily than apoE4 (74), suggesting that it may be more efficiently stimulated by HDL or apoA-I to enter the recycling pathway. Recently, expression of apoE4 in neurons was shown to impair glutamate receptor function and apoer2 receptor recycling by sequestering N-methyl-D-aspartate (NMDA), 2-amino-3-(5-methyl-3-oxo-1,2-oxazol-4-yl)propanoic acid (AMPA), and apo E receptor 2 (ApoER2) receptors intracellularly, thereby reducing their cell surface expression (75). As such, Reelin-induced long-term potentiation (LTP) is reduced, ultimately leading to impaired synaptic plasticity (75). Our results show that apoA-I stimulation of apoE recycling in glia increases LDLR levels in WT and ABCA1$^{-/-}$ glia. Future studies will address whether apoA-I can rescue impaired recycling of receptors in apoE4-expressing cells.

Another question raised by our study is whether stimulating apoE recycling may be beneficial or detrimental with respect to Aβ clearance and AD pathogenesis. On the one hand, increasing apoE recycling may promote brain RCT and elevate glutamate receptor levels. Stimulation of recycling may correct the relative deficit of apoE4 in the brain and CSF, as the net levels of apoE4 are lower in brain, CSF, and plasma of human apoE4-targeted replacement mice compared with apoE2 and apoE4 controls (76). Several other human and animal studies have also reported reduced apoE4 levels in the brain (77–81), but this is not always observed (82–84). On the other hand, our data would suggest that recycled apoE emerges as a lipid-poor particle that, unless rapidly lipidated by ABCA1, would be expected to promote amyloidogenesis (25, 26, 85). Finally, nothing is known about whether the various apoE lipoprotein particles secreted by glia vary in their interactions with Aβ or how such interactions may or may not affect lipoprotein function in RCT. Although much remains to be learned about how apoE functions in the healthy and diseased brain, continued activity in this research area may offer ways to overcome the detrimental aspects of apoE4 for both acute and chronic neurological conditions.

REFERENCES

1. Lund-Katz, S., and M. C. Phillips. 2010. High density lipoprotein structure-function and role in reverse cholesterol transport. *Subcell. Biochem.* **51:** 183–227.
2. Brooks-Wilson, A., M. Marcil, S. M. Clee, L. Zhang, K. Roomp, M. van Dam, L. Yu, C. Brewer, J. A. Collins, H. O. F. Molhuizen, et al. 1999. Mutations in ABC1 in Tangier disease and familial high-density lipoprotein deficiency. *Nat. Genet.* **22:** 336–345.
3. Rust, S., M. Rosier, H. Funke, Z. Amoura, J-C. Piette, J-F. Deleuze, H. B. Brewer, Jr., N. Duverger, P. Denèfle, and G. Assmann. 1999. Tangier disease is caused by mutations in the gene encoding ATP-binding cassette transporter 1. *Nat. Genet.* **22:** 352–355.
4. Bodzioch, M., E. Orsó, J. Klucken, T. Langmann, A. Böttcher, W. Diederich, W. Drobnik, S. Barlage, C. Büchler, M. Porsch-Özcürümez, et al. 1999. The gene encoding ATP-binding cassette transporter 1 is mutated in Tangier disease. *Nat. Genet.* **22:** 347–351.
5. Hirsch-Reinshagen, V., S. Zhou, B. L. Burgess, L. Bernier, S. A. McIsaac, J. Y. Chan, G. H. Tansley, J. S. Cohn, M. R. Hayden, and C. L. Wellington. 2004. Deficiency of ABCA1 impairs apolipoprotein E metabolism in brain. *J. Biol. Chem.* **279:** 41197–41207.
6. Wahrle, S. E., H. Jiang, M. Parsadanian, J. Legleiter, X. Han, J. D. Fryer, T. Kowalewski, and D. M. Holtzman. 2004. ABCA1 is required for normal CNS apoE levels and for lipidation of astrocyte-secreted apoE. *J. Biol. Chem.* **279:** 40987–40993.
7. Fredrickson, D. S., P. H. Altrocchi, L. V. Avioli, D. W. S. Goodman, and H. C. Goodman. 1961. Tangier disease: combined clinical staff conference at the National Institutes of Health. *Ann. Intern. Med.* **55:** 1016–1031.
8. Dietschy, J. M., and S. D. Turley. 2001. Cholesterol metabolism in the brain. *Curr. Opin. Lipidol.* **12:** 105–112.
9. Fan, J., J. Donkin, and C. L. Wellington. 2009. Greasing the wheels of Aβ clearance in Alzheimer's disease: the role of lipids and apolipoprotein E. *Biofactors.* **35:** 239–248.
10. Chattopadhyay, A., and Y. D. Paila. 2007. Lipid-protein interaction, regulation and dysfunction of brain cholesterol. *Biochem. Biophys. Res. Commun.* **354:** 627–633.
11. Vanier, M. T. 2010. Neimann-Pick disease type C. *Orphanet J. Rare Dis.* **5:** 16.
12. Ladu, M. J., C. Reardon, L. Van Eldik, A. M. Fagan, G. Bu, D. Holtzmann, and G. S. Getz. 2000. Lipoproteins in the central nervous system. *Ann. N. Y. Acad. Sci.* **903:** 167–175.
13. Pitas, R. E., J. K. Boyles, S. H. Lee, D. Hui, and K. H. Weisgraber. 1987. Lipoproteins and their receptors in the central nervous system. *J. Biol. Chem.* **262:** 14352–14360.
14. Saito, K., M. Seishima, M. P. Heyes, H. Song, S. Fujigaki, S. Maeda, J. H. Vickers, and A. Noma. 1997. Marked increases in concentrations of apolipoproteins in the cerebrospinal fluid of poliovirus-infected macaques: relations between apolipoprotein concentrations and severity of brain injury. *Biochem. J.* **321:** 145–149.
15. Song, H., K. Saito, M. Seishima, A. Noma, K. Urakami, and K. Nakashima. 1997. Cerebrospinal fluid apoE and apoA-I concentrations in early- and late-onset Alzheimer's disease. *Neurosci. Lett.* **231:** 175–178.
16. Demeester, N., G. Castro, C. Desrumaux, C. De Geitere, J. C. Fruchart, P. Santens, E. Mulleners, S. Engelborghs, P. P. De Deyn, J. Vandekerckhove, et al. 2000. Characterization and functional studies of lipoproteins, lipid transfer proteins, and lecithin:cholesterol acyltransferase in CSF of normal individuals and patients with Alzheimer's disease. *J. Lipid Res.* **41:** 963–974.
17. Koch, S., N. Donarski, K. Goetze, M. Kreckel, H. J. Sturernburg, C. Buhmann, and U. Beisiegel. 2001. Characterization of four lipoprotein classes in human cerebrospinal fluid. *J. Lipid Res.* **42:** 1143–1151.
18. Linton, M. F., R. Gish, S. T. Hubl, E. Butler, C. Esquivel, W. I. Bry, J. K. Boyles, M. R. Wardell, and S. G. Young. 1991. Phenotypes of apoliprotein B and apolipoprotein E after liver transplantation. *J. Clin. Invest.* **88:** 270–281.
19. Ladu, M. J., S. M. Gilligan, J. R. Lukens, V. G. Cabana, C. A. Reardon, L. J. Van Eldik, and D. A. Holtzman. 1998. Nascent astrocyte particles differ from lipoproteins in CSF. *J. Neurochem.* **70:** 2070–2081.
20. Lee, C. Y., and G. E. Landreth. 2010. The role of microglia in amyloid clearance from the AD brain. *J. Neural Transm.* **117:** 949–960.
21. Mahley, R. W., and S. C. Jr.Rall. 2000. Apolipoprotein E: far more than a lipid transport protein. *Annu. Rev. Genomics Hum. Genet.* **1:** 507–537.
22. Bertram, L., C. M. Lill, and R. Tanzi. 2010. The genetics of Alzheimer disease: back to the future. *Neuron.* **68:** 270–281.
23. Corder, E. H., A. M. Saunders, W. J. Strittmatter, D. E. Schmechel, P. C. Gaskell, G. W. Small, A. D. Roses, J. L. Haines, and M. A. Pericak-Vance. 1993. Gene dose of apolipoprotein E type 4 and the risk of Alzheimer's disease in late onset families. *Science.* **261:** 921–923.
24. Corder, E. H., A. M. Saunders, N. J. Risch, W. J. Strittmatter, D. E. Schmechel, P. C. Gaskell, J. B. Rimmler, P. A. Locke, P. M. Conneally, K. E. Schmader, et al. 1994. Protective effect of apolipoprotein E type 2 for late onset Alzheimer disease. *Nat. Genet.* **7:** 180–184.
25. Hirsch-Reinshagen, V., L. F. Maia, B. L. Burgess, J. F. Blain, K. E. Naus, S. A. McIsaac, P. F. Parkinson, J. Y. Chan, G. H. Tansley, M. R. Hayden, et al. 2005. The absence of ABCA1 decreases soluble apoE levels but does not diminish amyloid deposition in two murine models of Alzheimer's disease. *J. Biol. Chem.* **280:** 43243–43256.
26. Wahrle, S. E., H. Jiang, M. Parsadanian, R. E. Hartman, K. R. Bales, S. M. Paul, and D. M. Holtzman. 2005. Deletion of Abca1

increases Abeta deposition in the PDAPP transgenic mouse model of Alzheimer disease. *J. Biol. Chem.* **280:** 43236–43242.

27. Koldamova, R. P., I. M. Lefterov, M. Staufenbiel, D. Wolfe, S. Huang, J. C. Glorioso, M. Walter, M. G. Roth, and J. S. Lazo. 2005. The liver X receptor ligand TO901317 decreases amyloid β production in vitro and in a mouse model of Alzheimer's disease. *J. Biol. Chem.* **280:** 4079–4088.

28. Wahrle, S. E., H. Jiang, M. Parsadanian, J. Kim, A. Li, A. Knoten, S. Jain, V. Hirsch-Reinshagen, C. L. Wellington, K. R. Bales, et al. 2008. Overexpression of ABCA1 reduces amyloid deposition in the PDAPP mouse model of Alzheimer disease. *J. Clin. Invest.* **118:** 671–682.

29. Jiang, Q., C. Y. Lee, S. Mandrekar, B. Wilkinson, P. Cramer, N. Zelcer, K. Mann, B. Lamb, T. M. Willson, J. L. Collins, et al. 2008. ApoE promotes the proteolytic degradation of Abeta. *Neuron.* **58:** 681–693.

30. Verghese, P. B., J. M. Castellano, and D. M. Holtzman. 2011. Apolipoprotein E in Alzheimer's disease and other neurological disorders. *Lancet Neurol.* **10:** 241–252.

31. Rothblat, G. H., and M. C. Phillips. 2010. High-density lipoprotein heterogeneity and function in reverse cholesterol transport. *Curr. Opin. Lipidol.* **21:** 229–238.

32. Cavigiolio, G., B. Shao, E. G. Geier, G. Ren, J. W. Heinecke, and M. N. Oda. 2008. The interplay between size, morphology, stability, and functionality of high-density lipoprotein subclasses. *Biochemistry.* **47:** 4770–4779.

33. Timmins, J. M., J. Y. Lee, E. Boudyguina, K. D. Kluckman, L. R. Brunham, A. Mulya, A. K. Gebre, J. M. Coutinho, P. L. Colvin, T. L. Smith, et al. 2005. Targeted inactivation of hepatic Abca1 causes profound hypoalphalipoproteimemia and kidney hypercatabolism of apoA-I. *J. Clin. Invest.* **115:** 1333–1342.

34. Brunham, L. R., J. K. Kruit, J. Iqbal, C. Fievet, J. M. Timmins, T. D. Pape, B. A. Coburn, N. Bissada, B. Staels, A. K. Groen, et al. 2006. Intestinal ABCA1 directly contributes to HDL biogenesis in vivo. *J. Clin. Invest.* **116:** 1052–1062.

35. Asztalos, B. F., E. J. Schaefer, K. V. Horvath, S. Yamashita, M. Miller, G. Franceschini, and L. Calabresi. 2007. Role of LCAT in HDL remodeling: investigation of LCAT deficiency states. *J. Lipid Res.* **48:** 592–599.

36. Acton, S., A. Rigotti, K. T. Landschulz, S. Xu, H. H. Hobbs, and M. Krieger. 1996. Identification of scavenger receptor SR-BI as a high density lipoprotein receptor. *Science.* **271:** 518–520.

37. Fagan, A. M., D. M. Holtzman, G. Munson, T. Mathur, D. Schnieder, L. K. Chang, G. S. Getz, C. A. Reardon, J. Lukens, J. A. Shah, et al. 1999. Unique lipoproteins secreted by primary astrocytes from wild type, wild type, apoE (-/-), and human apoE transgenic mice. *J. Biol. Chem.* **274:** 30001–30004.

38. DeMattos, R. B., R. P. Brendza, J. E. Heuser, M. Kierson, J. R. Cirrito, J. Fryer, P. M. Sullivan, A. M. Fagan, X. Han, and D. A. Holtzman. 2001. Purification and characterization of astrocyte-secreted apolipoprotein E and J-containing lipoproteins from wild-type and human apoE transgenic mice. *Neurochem. Int.* **39:** 415–425.

39. Hirsch-Reinshagen, V., and C. L. Wellington. 2007. Cholesterol metabolism, apolipoprotein E, adenosine triphosphate-binding cassette transporters, and Alzheimer's disease. *Curr. Opin. Lipidol.* **18:** 325–332.

40. McNeish, J., R. J. Aiello, D. Guyot, T. Turi, C. Gabel, C. Aldinger, K. L. Hoppe, M. L. Roach, L. J. Royer, J. de Wet, et al. 2000. High density lipoprotein deficiency and foam cell accumulation in mice with targeted disruption of ATP-binding cassette transporter-1. *Proc. Natl. Acad. Sci. USA.* **97:** 4245–4250.

41. Ryan, R. O., T. M. Forte, and M. N. Oda. 2003. Optimized bacterial expression of human apolipoprotein A-I. *Protein Expr. Purif.* **27:** 98–103.

42. Rensen, P. C. N., M. C. Jong, L. C. van Vark, H. van der Boom, W. L. Hendricks, T. J. C. van Berkel, E. A. L. Biessen, and L. M. Havekes. 2000. Apolipoprotein E is resistant to intracellular degradation in vitro and in vivo. *J. Biol. Chem.* **275:** 8564–8571.

43. Fazio, S., M. F. Linton, A. H. Hasty, and L. L. Swift. 1999. Recycling of apolipoprotein E in mouse liver. *J. Biol. Chem.* **274:** 8247–8253.

44. Fazio, S., M. F. Linton, and L. L. Swift. 2000. The cell biology and physiologic relevance of ApoE recycling. *Trends Cardiovasc. Med.* **10:** 23–30.

45. Swift, L. L., M. H. Farkas, A. S. Major, K. Valyi-Nagy, M. F. Linton, and S. Fazio. 2001. A recycling pathway for resecretion of internalized apolioprotien E in liver cells. *J. Biol. Chem.* **276:** 22965–22970.

46. Ladu, M. J., J. A. Shah, C. A. Reardon, G. S. Getz, G. Bu, J. Hu, L. Guo, and L. J. Van Eldik. 2000. Apolipoprotein E receptors mediate the effects of β-amyloid on astrocyte cultures. *J. Biol. Chem.* **275:** 33974–33980.

47. Braun, N. A., P. J. Mohler, K. H. Weisgraber, A. H. Hasty, M. F. Linton, P. G. Yancey, Y. R. Su, S. Fazio, and L. L. Swift. 2006. Intracellular trafficing of recycling apolipoprotein E in Chinese hamster ovary cells. *J. Lipid Res.* **47:** 1176–1186.

48. Heeren, J., T. Grewal, A. Laatsch, D. Rottke, F. Rinninger, C. Enrich, and U. Beisiegel. 2003. Recycling of apolipoprotein E is associated with cholesterol efflux and high density lipoprotein internalization. *J. Biol. Chem.* **278:** 14370–14378.

49. Heeren, J., U. Beisiegel, and T. Grewal. 2006. Apolipoprotein E recycling implications for dyslipidemia and atherosclerosis. *Arterioscler. Thromb. Vasc. Biol.* **26:** 442–448.

50. Hasty, A. H., M. R. Plummer, K. H. Weisgraber, M. F. Linton, R. Fazio, and L. L. Swift. 2005. The recycling of apolipoprotein E in macrophages: influence of HDL and apolipoprotein A-I. *J. Lipid Res.* **46:** 1433–1439.

51. Farkas, M. H., L. L. Swift, A. H. Hasty, M. F. Linton, and S. Fazio. 2003. The recycling of apolipoprotein E in primary cultures of mouse hepatocytes. *J. Biol. Chem.* **278:** 9412–9417.

52. Bencharif, K., L. Hoareau, R. K. Murumalla, E. Tamus, F. Tallet, R. G. Clerc, C. Gardes, M. Cesari, and R. Roche. 2010. Effect of apoA-I on cholesterol release and apoE secretion in human mature adipocytes. *Lipids Health Dis.* **9:** 75–84.

53. Dory, L. 1991. Regulation of apolipoprotein E secretion by high density lipoprotein 3 in mouse macrophages. *J. Lipid Res.* **32:** 783–792.

54. Dory, L. 1989. Synthesis and secretion of apoE in thioglycolate-elicited mouse peritoneal macrophages: effect of cholesterol efflux. *J. Lipid Res.* **30:** 809–816.

55. Rellin, L., J. Heeren, and U. Beisiegel. 2008. Recycling of apolipoprotein E is not associated with cholesterol efflux in neuronal cells. *Biochim. Biophys. Acta.* **1781:** 232–238.

56. Kockx, M., K-A. Rye, K. Gaus, C. M. Quinn, J. Wright, T. Sloane, D. Sviridov, Y. Fu, D. Sullivan, J. R. Burnett, et al. 2004. Apolipoprotein A-I-stimulated apolipoprotein E secretion from human macrophages is independent of cholesterol efflux. *J. Biol. Chem.* **279:** 25966–25977.

57. Catte, A., J. C. Patterson, M. K. Jones, W. G. Jerome, D. Bashtovyy, Z. Su, F. Gu, J. Chen, M. P. Aliste, S. C. Harvey, et al. 2006. Novel changes in discoidal high density lipoprotein morphology: a molecular dynamics study. *Biophys. J.* **90:** 4345–4360.

58. Zhang, L., J. Song, G. Cavigiolio, B. Y. Ishida, S. Zhang, J. P. Kane, K. H. Weisgraber, M. N. Oda, K. A. Rye, H. J. Pownall, et al. 2011. Morphology and structure of lipoproteins revealed by an optimized negative-staining protocol of electron microscopy. *J. Lipid Res.* **52:** 175–178.

59. Ladu, M. J., W. B. Stine, M. Narita, G. S. Getz, C. A. Reardon, and G. Bu. 2006. Self-assembly of HEK cell-secreted apoE particles resembes apoE enrichment of lipoproteins as a ligand for the LDL receptor-related protein. *Biochemistry.* **45:** 381–390.

60. Rensen, P. C., N. Herjgers, M. H. Netscher, S. C. Meskers, M. Van Eck, and T. J. Van Berkel. 1997. Particle size determines the specificity of apolipoprotein E-containing triglyceride-rich emulsions for the LDL receptor versus hepatic remnant receptor in vivo. *J. Lipid Res.* **38:** 1070–1084.

61. Farkas, M. H., K. H. Weisgraber, V. L. Shepherd, M. F. Linton, S. Fazio, and L. L. Swift. 2004. The recycling of apolipoprotein E and its amino-terminal 22 kDa fragment: evidence for multiple redundant pathways. *J. Lipid Res.* **45:** 1546–1554.

62. Heeren, J., T. Grewal, S. Jackle, and U. Beisiegel. 2001. Recycling of apolipoprotein E and lipoprotein lipase through endosomeal compartments in vivo. *J. Biol. Chem.* **276:** 42333–42338.

63. Takahashi, Y., and J. D. Smith. 1999. Cholesterol efflux to apolipoprotein A1 involves endocytosis and resecretion in a calcium-dependent pathway. *Proc. Natl. Acad. Sci. USA.* **96:** 11358–11363.

64. Neufeld, E. B., J. A. Stonick, S. J. Demosky, C. L. Knapper, C. A. Combs, A. Cooney, M. Comly, N. Dwyer, J. Blanchette-Mackie, A. T. Remaley, et al. 2004. The ABCA1 transporter modulates late endocytic trafficking. *J. Biol. Chem.* **279:** 15571–15578.

65. Denis, M., Y. D. Landry, and X. Zha. 2008. ATP-binding cassett A1-mediated lipidation of apoA-I occurs at the plasma membrane and not in the endocytic compartment. *J. Biol. Chem.* **283:** 16178–16186.

66. Lefterov, I., N. F. Fitz, A. A. Cronican, A. Fogg, P. Lefterov, R. Kodali, R. Wetze, and R. Koldamova. 2010. Apolipoprotein A-I

deficiency increases cerebral amyloid angiopathy and cognitive deficits in APP/PS1E9 mice. *J. Biol. Chem.* **285:** 36945–36957.

67. Lewis, T. L., D. Cao, H. Lu, R. A. Mans, Y. R. Su, L. Jungbauer, M. F. Linton, S. Fazio, M. J. Ladu, and L. Li. 2010. Overexpression of human apolipoprotein A-I preserves cognitive function and attenuates neuroinflammation and cerebral amyloid angiopathy in a mouse model of Alzheimer's disease. *J. Biol. Chem.* **285:** 36958–36968.

68. Fagan, A. M., E. Christopher, J. W. Taylor, M. Parsadanian, M. Spinner, M. Watson, J. D. Fryer, S. Wahrle, K. R. Bales, S. M. Paul, et al. 2004. ApoAI deficiency results in marked reductions in plasma cholesterol but no alterations in amyloid-beta pathology in a mouse model of Alzheimer's disease-like cerebral amyloidosis. *Am. J. Pathol.* **165:** 1413–1422.

69. Heeren, J., T. Grewal, A. Laatsch, N. Becker, F. Rinninger, K-A. Rye, and U. Beisiegel. 2004. Impaired recycling of apolipoprotein E4 is associated with intracellular cholesterol accumulation. *J. Biol. Chem.* **279:** 55483–55492.

70. Zhong, N., and K. H. Weisgraber. 2009. Understanding the association of apolipoprotein E4 with Alzheimer disease: clues from its structure. *J. Biol. Chem.* **284:** 6027–6031.

71. Zhong, N., G. Ramaswamy, and K. H. Weisgraber. 2009. Apolipoprotein E4 domain interaction induces endoplasmic reticulum stress and impairs astrocyte function. *J. Biol. Chem.* **284:** 27273–27280.

72. Hatters, D. M., M. S. Budamagunta, J. C. Voss, and K. H. Weisgraber. 2005. Modulation of apolipoprotein E structure by domain interaction. *J. Biol. Chem.* **280:** 34288–34295.

73. Morrow, J. A., D. M. Hatters, B. Lu, P. Hochti, K. A. Oberg, B. Rupp, and K. H. Weisgraber. 2002. Apolipoprotein E4 forms a molten globule. A potential basis for its association with disease. *J. Biol. Chem.* **277:** 50380–50385.

74. Dong, L-M., C. Wilson, M. R. Wardell, T. Simmons, R. W. Mahley, K. H. Weisgraber, and D. A. Agard. 1994. Human apolipoprotein E. Role of arginine 61 in mediating the lipoprotein preferences of the E3 and E4 isoforms. *J. Biol. Chem.* **269:** 22358–22365.

75. Chen, Y., M. S. Durakoglugil, X. Xian, and J. Herz. 2010. ApoE4 reduces glutamate receptor function and synaptic plasticity by selectively impairing ApoE receptor recycling. *Proc. Natl. Acad. Sci. USA.* **107:** 12011–12016.

76. Riddell, D. R., H. Zhou, K. Atchison, H. K. Warwick, J. Jefferson, L. Xu, S. Aschmies, Y. Kirksey, Y. Hu, E. Wagner, et al. 2008. Impact of apolipoprotein E (apoE) polymorphism on brain apoE levels. *J. Neurosci.* **28:** 11445–11453.

77. Bertrand, P., J. Poirier, T. Oda, C. E. Finch, and G. M. Pasinetti. 1995. Association of apolipoprotein E genotype with brain levels of apolipoprotein E and apolipoprotein J (clusterin) in Alzheimer dsiease. *Brain Res. Mol. Brain Res.* **33:** 174–178.

78. Beffert, U., J. S. Cohn, C. Petit-Turcotte, M. Tremblay, N. Aumont, C. Ramassamy, J. Davignon, and J. Poirier. 1999. Apolipoprotein E and beta-amyloid levels in the hippocampus and frontal cortex of Alzheimer's disease subjects are disease-related and apolipoprotein E genotype dependent. *Brain Res.* **843:** 87–94.

79. Poirier, J. 2005. Apolipoprotein E, cholesterol transport and synthesis in sporadic Alzheimer's disease. *Neurobiol. Aging.* **26:** 355–361.

80. Glockner, F., V. Meske, and T. G. Ohm. 2002. Genotype-related differences of hippocampal apolipoprotein E levels only in early stages of neuropathological changes in Alzheimer's disease. *Neuroscience.* **114:** 1103–1114.

81. Ramaswamy, G., Q. Xu, Y. Huang, and K. H. Weisgraber. 2005. Effect of domain interaction on apolipoprotein E levels in mouse brain. *J. Neurosci.* **25:** 10658–10663.

82. Fryer, J. D., K. Simmons, M. Parsadanian, K. R. Bales, S. M. Paul, P. M. Sullivan, and D. M. Holtzman. 2005. Human apolipoprotein E4 alters the amyloid-beta 40:42 ratio and promotes the formation of cerebral amyloid angiopathy in an amyloid precursor protein transgenic model. *J. Neurosci.* **25:** 2803–2810.

83. Sullivan, P. M., B. E. Mace, N. Maeda, and D. E. Schmechel. 2004. Marked regional differences of brain human apolipoprotein E expression in targeted replacement mice. *Neuroscience.* **124:** 725–733.

84. Fukumoto, H., M. Tennis, J. J. Locascio, B. T. Hyman, J. H. Growdon, and M. C. Irizarry. 2003. Age but not diagnosis is the main predictor of plasma amyloid β-protein levels. *Arch. Neurol.* **60:** 958–964.

85. Koldamova, R., M. Staufenbiel, and I. Lefterov. 2005. Lack of ABCA1 considerably decreases brain apoE level and increases amyloid deposition in APP23 mice. *J. Biol. Chem.* **280:** 43224–43235.